Calhoun: The NPS Institutional Archive

DSpace Repository

Theses and Dissertations | 1. Thesis and Dissertation Collection, all items

1988

Random wave forces on a free-to-surge vertical cylinder

Sajonia, Charles Blake

Monterey California. Naval Postgraduate School

https://hdl.handle.net/10945/23103

This publication is a work of the U.S. Government as defined in Title 17, United States Code, Section 101. Copyright protection is not available for this work in the United States.

Downloaded from NPS Archive: Calhoun

Calhoun is the Naval Postgraduate School's public access digital repository for research materials and institutional publications created by the NPS community. Calhoun is named for Professor of Mathematics Guy K. Calhoun, NPS's first appointed -- and published -- scholarly author.

Dudley Knox Library / Naval Postgraduate School
411 Dyer Road / 1 University Circle
Monterey, California USA 93943

http://www.nps.edu/library

DUDLEY KNOX LIBRARY
NAVAL POSTGRADUATE SCHOOL
MONTEREY, CA 93943-5002

RANDOM WAVE FORCES ON A FREE-TO-SURGE VERTICAL CYLINDER

A Thesis

by

CHARLES BLAKE SAJONIA

Submitted to the Graduate College of
Texas A&M University
in partial fulfillment of the requirements for the degree of

MASTER OF SCIENCE

May 1988

Major Subject: Ocean Engineering

RANDOM WAVE FORCES ON A FREE-TO-SURGE
VERTICAL CYLINDER

A Thesis

by

CHARLES BLAKE SAJONIA

Approved as to style and content by:

DUDLEY KNOX LIBRARY
NAVAL POSTGRADUATE SCHOOL
MONTEREY, CALIFORNIA 93943-5002

ABSTRACT

Random Wave Forces on a Free-to-Surge Vertical Cylinder (May 1988)

Charles Blake Sajonia, B.S., University of Washington

Chairman of Advisory Committee: Dr. J. M. Niedzwecki

The principal objective of this research is to to gain insight into the applications and limitations of the relative motion form of the Morison equation for the prediction of hydrodynamic forces on a free-to-surge vertical cylinder in random waves. Force transfer coefficients are estimated from experimental data using regression with auto-regressive errors. The best-fit relative motion form of the Morison equation results in a root-mean-square error of 24% and a multiple correlation coefficient of 0.71, over a 16 second time series. A high frequency force component not accounted for in the Morison equation is quantified. Cross-spectra are used to show that this residual force can not be duplicated by the relative motion Morison equation due to the lack of explicit history terms. A force transfer model containing explicit history terms is presented. The improvement in force prediction with increasing memory is illustrated and a memory length is chosen that optimizes the tradeoff between model complexity and goodness-of-fit. The new model reduces the rms error from 24% to 9%, increases the multiple correlation coefficient from 0.71 to 0.83, and captures the high frequency force components not accounted for in the Morison equation. A simple numerical simulation of a tension leg platform is performed to illustrate the application and limitations of the results.

To my wife, Kelly.

ACKNOWLEDGMENTS

The author is grateful to his committee chair, Dr. John M. Niedzwecki, and members, Dr. H. Joseph Newton and Dr. Robert E. Randall, for their guidance, constructive criticisms, and encouragement throughout this research. Mr. David R. Shields of the Naval Civil Engineering Laboratory is gratefully acknowledged for his assistance in the selection of a thesis topic and for his valuable comments throughout this research. Dr. Thomas H. Dawson of the U.S. Naval Academy, Naval System Engineering Department, and Ms. Louise A. Wallendorf of the U.S. Naval Academy, Hydromechanics Laboratory are gratefully acknowledged for allowing the author to participate in their experimental program. Finally, the author is grateful to Captain Donald R. Wells, CEC, USN, Commanding Officer of the Naval Civil Engineering Laboratory, for selecting him for the Naval Facilities Engineering Command (NAVFAC) Ocean Facilities Program.

TABLE OF CONTENTS

CHAPTER		Page
I	INTRODUCTION	1
	A. The Relative Motion Morison Equation	1
	B. Flow History	2
	C. Regression Analysis	5
	D. U.S. Naval Academy Experimental Program	6
II	DATA ANALYSIS	9
	A. Fluid Particle Kinematics	9
	B. Regression Model Formulation and Solution	10
	C. The Best-Fit Relative Motion Morison Equation	11
	D. A Force Transfer Model with Memory	17
	E. Model Complexity vs. Goodness-of-Fit	18
III	NUMERICAL SIMULATION	26
	A. Tension Leg Platform Model	26
	B. Solution Procedure	30
	C. Simulation Results	31
IV	CONCLUSIONS	44
	REFERENCES	45
	APPENDIX A: NOMENCLATURE	47
	APPENDIX B: TIME SERIES ANALYSIS SOFTWARE	50
	VITA	53

LIST OF FIGURES

Figure		Page
1.	Sketch of U.S. Naval Academy Test Assembly	8
2.	Best-Fit Relative Motion Morison Equation	12
3.	Spectral Density: Morison Equation	14
4.	Coherency Spectra: Independent & Dependent Vectors	15
5.	Phase Spectra: Independent & Dependent Vectors	16
6.	Zero Lag Memory	20
7.	Five Lag Memory	21
8.	Ten Lag Memory	22
9.	Fifteen Lag Memory	23
10.	Twenty Lag Memory	24
11.	Spectral Density: Ten Lag Memory	25
12.	Schematic of a Tension Leg Platform	27
13.	Tension Leg Platform Restoring Force	29
14.	Response Simulation Flow Chart	32
15.	Surface Elevation – Case One	34
16.	Force Using Morison Equation – Case One	35
17.	Force Using Filters – Case One	36
18.	TLP Surge Response – Case One	37
19.	TLP Tension – Case One	38
20.	Surface Elevation – Case Two	39
21.	Force Using Morison Equation – Case Two	40
22.	Force Using Filters – Case Two	41
23.	TLP Surge Response – Case Two	42
24.	TLP Tension – Case Two	43

CHAPTER I

INTRODUCTION

A. The Relative Motion Morison Equation

The principle objective of this research is to gain insight into the applications and limitations of the relative motion form of the Morison equation for the prediction of hydrodynamic forces on a free-to-surge vertical cylinder in random waves. In 1950 Morison, O'Brien, Johnson, and Schaaf (1950) presented an empirical equation which describes the wave induced hydrodynamic loading on a fixed vertical pile. Their equation, which is popularly known as the Morison equation, can be expressed as

$$f = C_d \rho \frac{D}{2} |u| u + C_m \rho \frac{\pi D^2}{4} a, \tag{1.1}$$

where f is the force per unit length acting on the pile, C_d and C_m are force transfer coefficients, u and a are the horizontal fluid particle velocity and acceleration, ρ is the density of the fluid, and D is the diameter of the pile or cylinder. The total wave induced force acting on the cylinder is considered as the sum of a viscous drag force component and an inertia component. When the structure moves in response to hydrodynamic loads, Equation (1.1) is often modified by using relative velocities and accelerations. The resulting equation is known as the relative motion or wave-structure interaction form of the Morison equation. This equation can be expressed as

$$f = C_d \rho \frac{D}{2} |u - \dot{x}| (u - \dot{x}) + C_a \rho \frac{\pi D^2}{4} (a - \ddot{x}) + \rho \frac{\pi D^2}{4} a, \tag{1.2}$$

Journal model is *ASCE Proceedings of the Waterway, Port, Coastal and Ocean Engineering Division.*

where $\dot{x}$ and $\ddot{x}$ are the velocity and acceleration of the cylinder, respectively, C_a is the added mass coefficient defined as $C_a = C_m - 1$, and the last term is known as the Froude-Krylov force which is the result of the local acceleration of the unsteady flow.

A number of researchers, e.g. (Sarpkaya and Isaacson, 1981), have shown that the force transfer coefficients C_d and C_m are not simple constants, but functions of at least four parameters: cylinder roughness, Reynolds number, Keulegan-Carpenter number, and time. Thus, the relative motion Morison equation is an engineering approximation to a complex problem.

B. Flow History

Although the Morison equation contains only instantaneous or time averaged parameters, the actual hydrodynamic force acting on a submerged body depends on both the instantaneous and preceding flow conditions (Hamiliton, 1972). However, most investigators have ignored this history dependence in light of the many other uncertainties in wave force calculations. Others, such as Keulegan and Carpenter (1958) and Sarpkaya (1981) have corrected for this error by including an instantaneous correction term. In periodic flow, the fluid particle kinematics change with time, but the pattern is continually repeated. Since the preceding cycles are identical, the history effects can be represented by an instantaneous correction term instead of an explicit history term. This approach was utilized by Keulegan and Carpenter (1958) in a series of seiche-tank flow experiments. A "remainder force" ΔR was introduced to account for the differences between predicted and measured forces on a submerged cylinder.

Sarpkaya (1981) has also quantified ΔR in a series of one-dimensional periodic

flow experiments. In addition, the limitations of the Morison equation were illustrated by plotting the instantaneous values of C_d and C_m. It was shown that C_d and C_m exhibit large variations during a given cycle, particularly for values of the Keulegan-Carpenter number between 8 and 25, and that accelerating and decelerating flows, with identical absolute values of the corresponding fluid particle kinematics, do not exert identical forces on the cylinder. These observations suggest that ΔR is partly the result of neglecting the effects of flow history and partly due to the other simplifications inherent in the Morison equation. Sarpkaya represented the "remainder force" as an instantaneous correction term given by the Fourier expansion proposed by Keulegan and Carpenter (1958), or

$$\Delta R = C_3 \cos(3\theta - \phi_3) + C_5 \cos(5\theta - \phi_5) + \ldots + C_n \cos(n\theta - \phi_n), \tag{1.3}$$

where $\theta = \frac{2\pi t}{T}$. The use of odd harmonics was justified since the significant force components occurred at the fundamental frequency and the 3rd and 5th harmonics. The force transfer model proposed by Keulegan and Carpenter (1958) and Sarpkaya (1981) is then the sum of Equations (1.1) and (1.3), or

$$f = C_d \rho \frac{D}{2} |u| u + C_m \rho \frac{\pi D^2}{4} a + C_3 \cos(3\theta - \phi_3) + C_5 \cos(5\theta - \phi_5), \tag{1.4}$$

where $u = -U \cos\theta$, i.e. the flow is periodic with a maximum velocity equal to U. Although this model reduces the rms residual force by approximately 60%, it has two limitations: (1) the four parameters which define the correction term C_3, C_5, ϕ_3 and ϕ_5 have little physical significance, and (2) the flow is assumed to be periodic. The experiments performed by Keulegan and Carpenter (1958) and Sarpkaya (1981) prove that ΔR is not the result of the complications introduced in wavy flow, e.g. the limitations of the wave theory employed to estimate the fluid

particle kinematics, the orbital fluid particle motion, etc. Therefore, attempts to correct for this error by adjusting the wave theory model may not lead to significant improvement.

Bird and Mockros (1986) performed a series of 28 tests in which an instrumented cylinder was accelerated or decelerated in still water in order to estimate the relative magnitude of the history force. Four cases were examined: (1) acceleration from rest to a constant velocity, (2) deceleration from a constant velocity to rest, (3) acceleration from one constant velocity to a higher constant velocity and (4) reversal from a constant velocity to a similar constant velocity in the opposite direction. The results verify the findings of Sarpkaya (1981) and suggest that the relative magnitude of the history force is significant, and at times equal to the maximum added mass force during acceleration and over half the steady state drag force during deceleration for the specific cases studied. The method employed by Bird and Mockros (1986) to estimate the history force was somewhat arbitrary since it was presumed that the Morison equation, with constant coefficients, can correctly predict the instantaneous drag and inertia components. Bird and Mockros proposed that the introduction of a history force term may account for an important feature of the fluid dynamics and reduce the variability between measured and calculated forces. The force subdivision approach was based on a discussion given by Hamilton (1972). Hamilton suggested that the hydrodynamic force on a submerged body in nonperiodic flow should be separated into three parts:

(1) the conventional drag component,

(2) the conventional inertia component, and

(3) an explicit history term.

C. Regression Analysis

Given the time varying force acting on a cylinder and the corresponding fluid particle kinematics, force transfer coefficients may be estimated in a variety of ways. The approach employed by most researchers in the past has been ordinary least squares regression, e.g. Reid (1958), Aagaard and Dean (1969), and Wheeler (1970). However, new statistical techniques are now available which are particularly suitable for time series data (Newton, 1988). Therefore, a brief review of regression analysis and an alternative model fitting technique are presented.

Regression analysis is the fitting of an equation to a set of values. The equation predicts the response vector y from a function of the regressor matrix X and parameter vector B, adjusting the parameters such that a measure of fit is optimized. The method used to estimate the parameters is to minimize the sum of the squares of the differences between the actual and predicted responses. In matrix notation

$$y = XB + \epsilon, \tag{1.5}$$

such that B minimizes

$$S(B) = (y - XB)^T(y - XB). \tag{1.6}$$

This analysis is based on several assumptions, including: (1) that the expected value of the errors (ϵ) is zero and (2) that the errors are uncorrelated across observations. When regression is performed on time series data, the errors are often autocorrelated, violating the second assumption and perhaps the first. In this case there are several new methods to estimate B. One such method is regression with autoregressive (AR) errors. This is an iterative procedure in which the following steps are performed:

(1) use ordinary least squares to find initial estimates of B and ϵ,

(2) fit an AR model to ϵ,

(3) create a new response vector z and regressor matrix W by applying the AR filter of step (2) and

(4) return to step (1) using z and W instead of y and X.

This process is repeated until successive iterations result in the same value of AR order. A more thorough discussion along with the software required to perform the above analysis is given by Newton (1988).

D. U.S. Naval Academy Experimental Program

In order to gain insight into the applications and limitations of the relative motion form of the Morison equation, a multiple phase experimental program was conducted at the U.S. Naval Academy, Hydromechanics Laboratory (Shields and Hudspeth, 1985). The results from the earlier phases are reported by Dawson (1984) and Dawson, Wallendorf and Hill (1986). The data analyzed in this thesis is the result of an extension of these experiments to include both relative motion and random wave loading. The USNA test assembly was subjected to random waves of approximate Bretschneider spectra with a significant wave height of 20 cm and a dominant wave period of 2.38 seconds. The maximum Reynolds number was approximately 2×10^4 and the maximum Keulegan-Carpenter number was approximately 50.

The test assembly consisted of a smooth stainless steel rod of one meter length and 2.54 cm diameter. The cylinder is attached to a free-to-surge aluminum subcarriage which is supported on two linear bearings and restrained be elastic springs. The test assembly is illustrated in Figure 1. Instrumentation used in the

experiments included a high frequency sonic transducer, a variable reluctance force gage and a resistance wave staff. Instrument signals were passed through an analog filter with 20 Hz cut-off frequency and an analog-to-digital converter before storing on computer disk. The acquisition rate was 51.2 samples per second. The accuracy of the measured surface elevation, surge displacement, and force are estimated to be 0.02 cm, 0.02 cm, and 0.05 N, respectively (Dawson, Wallendorf and Hill, 1986). The data is analyzed in the next chapter using time series analysis techniques.

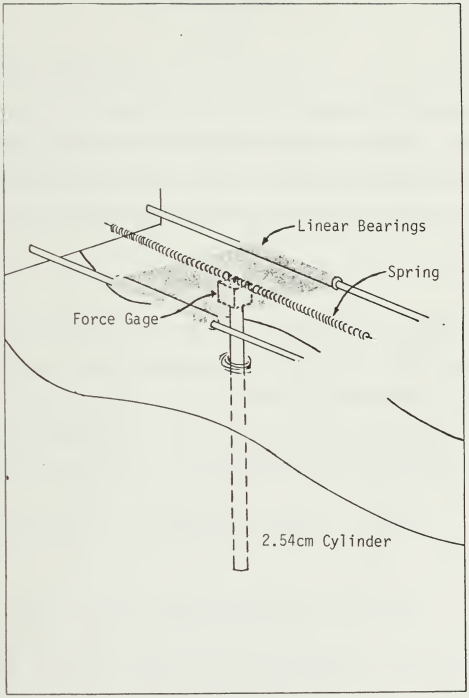

Figure 1. Sketch of U.S. Naval Academy Test Assembly.

CHAPTER II

DATA ANALYSIS

A. Fluid Particle Kinematics

The first step in analyzing the USNA data is to estimate the fluid particle kinematics from the measured surface elevation time series. This is accomplished using harmonic analysis. The measured surface elevation is represented as an infinite sum of small amplitude waves, with closely spaced frequencies, and random phase angles

$$\eta(x,t) = \sum_{n=1}^{\infty} A_n \cos(k_n x - \omega_n t + \phi_n), \tag{2.1}$$

where η denotes the elevation of the water surface above the mean water level, A_n is the amplitude of the nth wave component, and k_n, ω_n, and ϕ_n are the corresponding wave number, frequency, and phase (Borgman, 1972). The amplitudes A_n and phase angles ϕ_n are calculated most efficiently using the fast Fourier transform (FFT) algorithm. The horizontal velocity and acceleration at (x,z,t) are then given by

$$u(x,z,t) = \sum_{n=1}^{\infty} \omega_n \frac{\cosh k_n(h+z)}{\sinh k_n h} A_n \cos(kx - \omega_n t + \phi_n), \tag{2.2}$$

and

$$a(x,z,t) = \sum_{n=1}^{\infty} \omega_n^2 \frac{\cosh k_n(h+z)}{\sinh k_n h} A_n \sin(kx - \omega_n t + \phi_n), \tag{2.3}$$

where the wave number and frequency are related through the dispersion relation

$$\omega_n^2 = g k_n \tanh k_n h. \tag{2.4}$$

In Equations (2.1) through (2.3) the Fourier components are summed from $n = 1$ to ∞, however, wave records generally consist of discrete samples. A sampling

interval of 1/10th to 1/20th of the dominant wave period is often recommended. The highest frequency that can be used in the Fourier summation is then

$$f_0 = \frac{0.5}{\Delta t}, \tag{2.5}$$

where Δt is the sampling interval. This frequency is known as the Nyquist frequency. The dominant wave period of the USNA data is 2.38 seconds. A sampling interval of approximately 1/15th of the dominant wave period was chosen, or $\Delta t = 0.15624$ seconds. Therefore, the Nyquist frequency is approximately 3.2 Hz. This sampling interval reduces the amount of data to be processed without loss of any significant high frequency components. The spectral density estimates before and after sampling were compared to ensure that the measured spectra were represented accurately.

B. Regression Model Formulation and Solution

Given the time varying force acting on the cylinder, and the corresponding fluid particle kinematics and cylinder dispacement, force transfer coefficients can be estimated using the regression with AR-errors technique described in Chapter 1. The total force acting on the cylinder at time t may be considered as the linear combination of three terms: (1) the drag component F_D given by

$$F_D(t) = \rho \frac{D}{2} \int_{-h}^{0} \left| u(z,t) - \dot{x}(t) \right| \left\{ u(z,t) - \dot{x}(t) \right\} dz, \tag{2.6}$$

(2) the inertia component F_I given by

$$F_I(t) = \rho \frac{\pi D^2}{4} \int_{-h}^{0} \left\{ a(z,t) - \ddot{x}(t) \right\} dz, \tag{2.7}$$

and (3) a force component resulting from the acceleration of the fluid by the cylinder, F_F given by

$$F_F(t) = \rho \forall \ddot{x}(t), \tag{2.8}$$

where h is the submerged length of the cylinder and $\forall$ is the volume of displaced fluid. The last term may be combined with the measured force acting on the cylinder and denoted by $F(t)$ to give

$$F(t) = C_d F_D(t) + C_m F_I(t). \tag{2.9}$$

Equation (2.9) is now in the form of the regression model $y = XB + \epsilon$, where $X = (F_D, F_I)$ and $B = (C_d, C_m)^T$. The best linear unbiased estimate of B results in:

$$C_d = 0.93 \quad \text{and} \quad C_m = 1.73.$$

A thorough time series analysis of the errors results in the following observations: (1) the errors ϵ are highly autocorrelated, (2) the cross-correlations between the prewhitened error time series and the prewhitened cylinder velocity and surface elevation time series are relatively small (less than 0.4), and (3) the cross-correlation between the prewhitened error time series and the prewhitened measured force F is large (approximately 0.8 at lag zero). Based on these observations one may conclude that the errors are not the result of the extension of the Morison equation to include relative motion, but are indicative of a systematic modeling error in the original Morison equation. The primary source of this error is determined in the following section.

C. The Best-Fit Relative Motion Morison Equation

Figure 2 compares the best-fit relative motion Morison equation with the measured force over a 16 second realization. The Morison equation "tracks" the measured time series fairly well, but underpredicts the rms force by 21%.

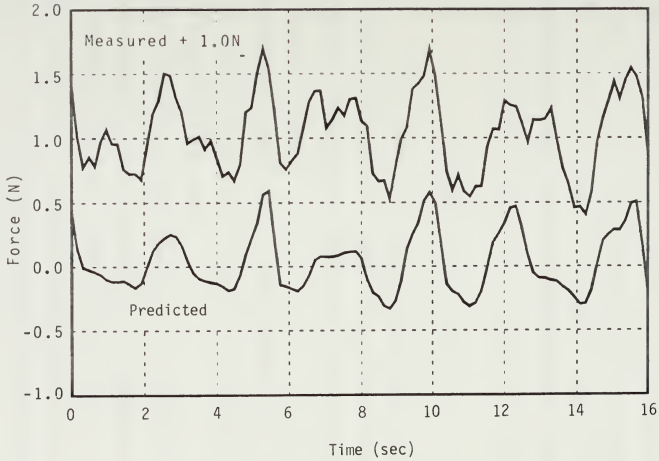

Figure 2. Best-Fit Relative Motion Morison Equation. Comparison of Measured and Predicted Force Realizations – RMS Error=21%, R^2=0.77.

The multiple correlation coefficient, defined as

$$R^2 = 1 - \frac{\sigma_\epsilon^2}{\sigma_y^2}, \tag{2.10}$$

where σ_ϵ^2 and σ_y^2 are the sample variance of the errors and the measured force realizations, is 0.77. One can see qualitatively, that the predicted time series is "smooth", while the measured time series is somewhat "wiggly". This is due to the presence of a series of high frequency force components that the Morison equation lacks. This discrepancy is illustrated using the standardized spectral density, defined as

$$\ln \frac{S_{11}(\omega)}{\sigma^2} \quad \text{versus} \quad \omega = \frac{k-1}{n} \tag{2.11}$$

for $k = 1, \ldots, [\frac{n}{2}] + 1$, where S_{11} is the usual two-sided spectral density, σ^2 is the sample variance, and n is the total number of observations (Newton, 1988). The standardized two-sided spectral density estimates for both predicted and measured forces are shown in Figure 3.

The high frequency residual force is readily apparent, with a peak at approximately five times the fundamental frequency. The cause of this error can be determined through cross-spectra analysis.

Recall that the drag and inertia components serve as the independent vectors in the regression model, while the measured force is the dependent vector. Figures 4 and 5 show the cross-spectra of the independent and dependent vectors.

Figure 4 is a graph of the coherency spectrum $W_{12}(\omega)$ which measures the relationship between the amplitudes of the sinusoids in the two univariate realizations at frequency ω. The coherence is given by

$$W_{12}(\omega) = \frac{|S_{12}(\omega)|}{\sqrt{S_{11}(\omega) S_{22}(\omega)}}, \tag{2.12}$$

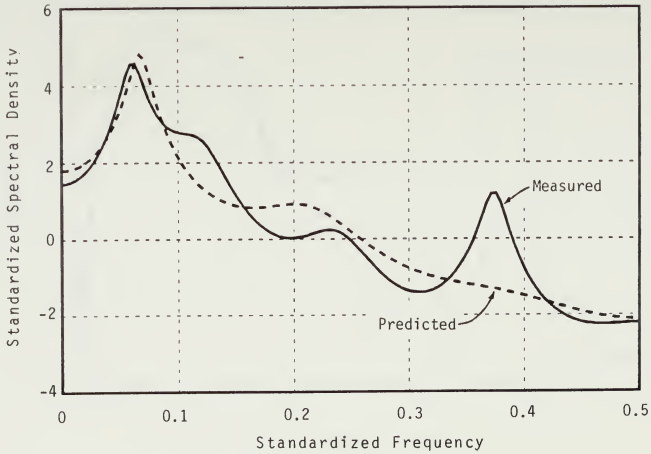

Figure 3. Spectral Density: Morison Equation. Comparison of Measured and Predicted Force Spectra Using the Relative Motion Morison Equation.

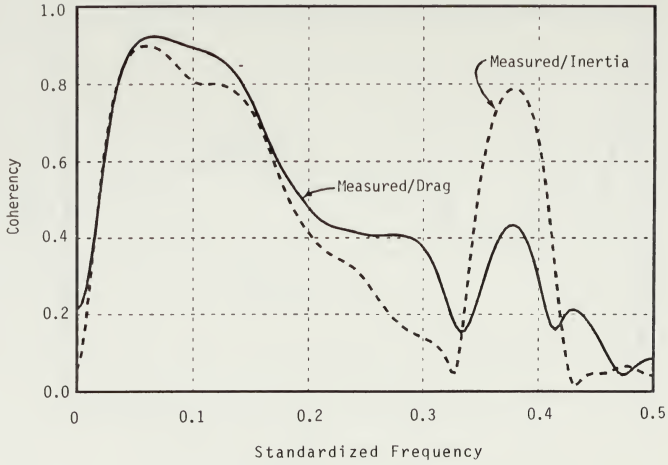

Figure 4. Coherency Spectra: Independent & Dependent Vectors. Significant Values Occur at Both the Fundamental and 5th Harmonic.

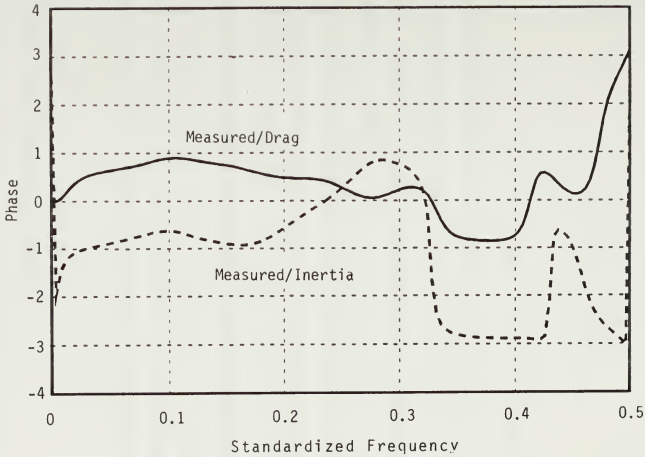

Figure 5. Phase Spectra: Independent & Dependent Vectors. The Fundamental and 5th Harmonic Are Out of Phase.

where S_{11} and S_{22} are the usual two-sided univariate spectral densities, and S_{12} is the complex cross-spectral density. Figure 5 is a graph of the phase spectrum $\phi_{12}(\omega)$ which measures how out of phase the frequency components for the univariate realizations tend to be. The phase is given by

$$\phi_{12}(\omega) = \tan^{-1} -\{\frac{q_{12}(\omega)}{c_{12}(\omega)}\}, \tag{2.13}$$

where

$$c_{12}(\omega) = \mathrm{Re}\,\{S_{12}(\omega)\} \quad \text{and} \quad q_{12}(\omega) = \text{-}\mathrm{Im}\,\{S_{12}(\omega)\}, \tag{2.14}$$

are the cospectral density and the quadrature spectral density, respectively.

Two important observations can be made from the cross-spectra: (1) the coherence is significant at both the fundamental and 5th harmonic, and (2) a considerable phase shift exists between the fundamental and the 5th harmonic. Since the relative motion Morison equation, which contains only instantaneous and time averaged parameters, is able to capture the fundamental frequency component, but not the 5th harmonic, one may conclude that the 5th harmonic lags the fundamental frequency component. That is, the 5th harmonic is the result of flow history. If this is true, then considerable improvement in force prediction can be achieved through the use of a force transfer model containing lagged versions of the independent vectors, i.e. history terms. Such a model is presented in the next section.

D. A Force Transfer Equation with Memory

Recall that the regression model used to estimate the best-fit relative motion Morison equation is

$$F(t) = C_d F_D(t) + C_m F_I(t). \tag{2.15}$$

Instead of the usual approach of using time averaged force transfer coefficients C_d and C_m, consider $F(t)$ as the sum of a filtered version of the drag component time series plus a filtered version of the inertia component time series, or

$$F(t) = \sum_{k=-\infty}^{\infty} \alpha_k F_D(t-k) + \sum_{k=-\infty}^{\infty} \beta_k F_I(t-k), \tag{2.16a}$$

with the following constraints

$$\alpha_k = \begin{cases} 0, & \text{if } k < 0; \\ 0, & \text{if } k > l \end{cases} \quad \text{and} \quad \beta_k = \begin{cases} 0, & \text{if } k < 0; \\ 0, & \text{if } k > l \end{cases} \tag{2.16b}$$

where α and β are force transfer coefficient vectors, and l is the maximum lag used in the model, i.e. l is a measure of the memory. Note that when $l = 0$ Equation (2.16) reduces to Equation (2.15), the relative motion Morison equation. Thus, the instantaneous force acting on the cylinder is now represented by the superposition of a filtered version of the drag component and a filtered version of the inertia component, both containing only non-negative lags. In this thesis, Equation (2.16) will be called the "force transfer filters". The improvement in force prediction, and the tradeoff between model complexity and goodness-of-fit is illustrated in the next section.

E. Model Complexity vs. Goodness-of-Fit

Figures 6 through 10 illustrate the improvement in force prediction with increasing memory. As the memory is increased, the error between rms forces is reduced while the multiple correlation coefficient R^2 is increased. These calcualtions were performed on 27 realizations containing a total of 432 seconds of data (approximately 180 waves). As is the case with most regression models, there is a tradeoff between model complexity and goodness-of-fit. For the USNA data a

ten lag memory was chosen as the optimal model. Using the force transfer filters with $l = 10$ reduces the mean rms error from 24% to 9% while increasing the mean multiple correlation coefficient from 0.71 to 0.83. Since the sampling interval is $\Delta t = 0.15624$ seconds, the 10 lag memory corresponds to 1.5624 seconds. This can be nondimensionalized by dividing by the dominant wave period $T = 2.38$ seconds to give

$$\Delta t \frac{l}{T} = 0.66.$$

Thus, the optimal model for the USNA data contains a memory equal to two thirds of the dominant wave period.

In addition to decreasing the rms residual force by an average of 170%, the force transfer filters capture the 5th harmonic not accounted for in the Morison equation. These small amplitude, high frequency force components may govern the fatigue analysis of offshore structures. As shown in Figure 11, the ten lag memory force transfer filters duplicate the measured spectral density almost exactly.

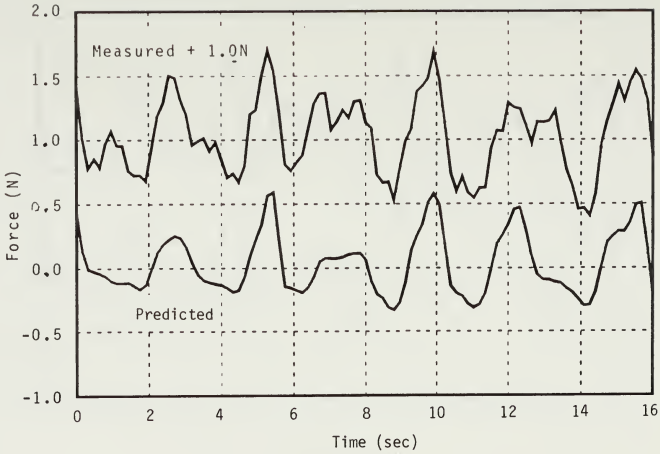

Figure 6. Zero Lag Memory. (Morison equation.) Comparison of Measured and Predicted Force Realizations – RMS Error=21%, R^2=0.77.

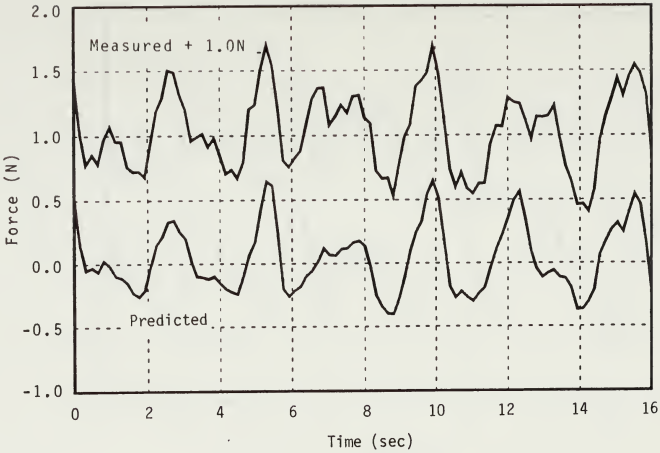

Figure 7. Five Lag Memory. Comparison of Measured and Predicted Force Realizations Using the Force Transfer Filters – RMS Error=13%, R^2=0.82.

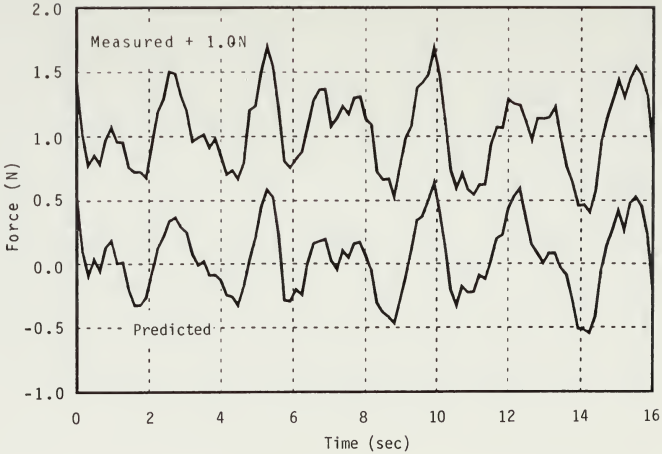

Figure 8. Ten Lag Memory. Comparison of Measured and Predicted Force Realizations Using the Force Transfer Filters – RMS Error=6%, R^2=0.86.

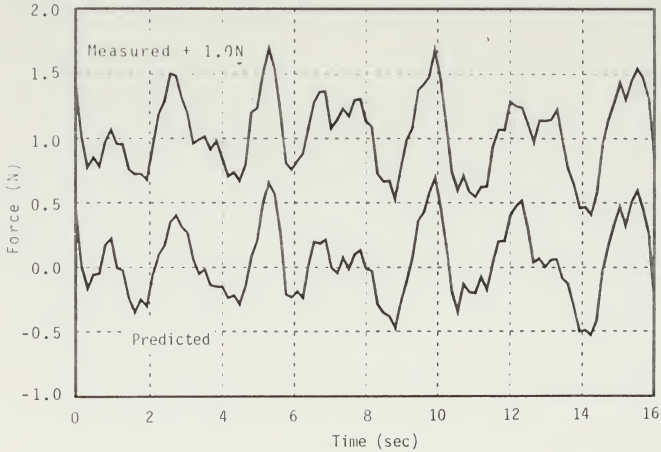

Figure 9. Fifteen Lag Memory. Comparison of Measured and Predicted Force Realizations Using the Force Transfer Filters - RMS Error=5%, R^2=0.87.

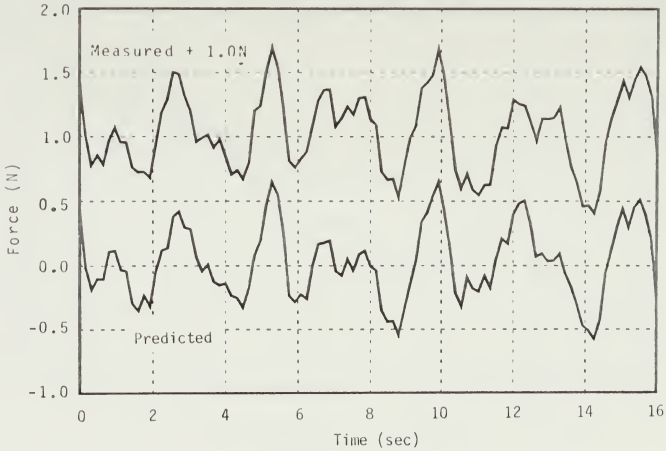

Figure 10. Twenty Lag Memory. Comparison of Measured and Predicted Force Realizations Using the Force Transfer Filters – RMS Error=5%, R^2=0.87.

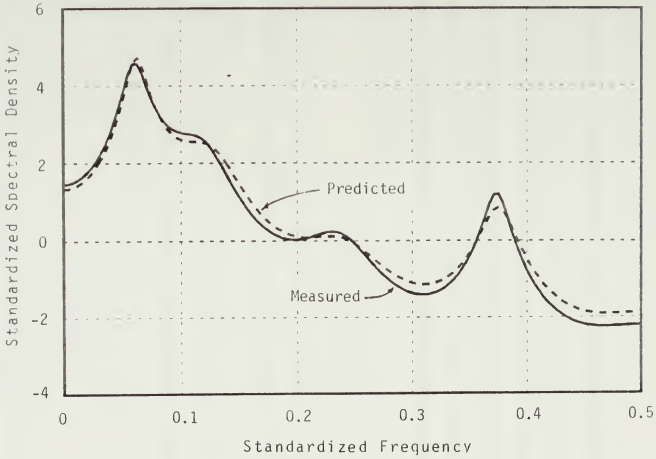

Figure 11. Spectral Density: Ten Lag Memory. Comparison of Measured and Predicted Force Spectra Using the Force Transfer Filters.

CHAPTER III

NUMERICAL SIMULATION

A. Tension Leg Platform Model

The purpose of this chapter is to provide a simple example of the application of the force transfer models discussed in Chapter 2. A tension leg platform is modeled as a nonlinear, single degree of freedom system (SDOFS) by considering motion only in the surge direction. Riser and tendon dynamics are neglected. Furthermore, it is assumed that diffraction and reflection of the waves are negligible. The equation of motion is established by equating the sum of the inertia, damping, stiffness and external forces at time t_i:

$$m\ddot{x}_i + c\dot{x}_i + kx = F_i, \tag{3.1}$$

where m is the mass of the platform and deck equipment, c is the damping, k is the stiffness and F_i is the hydrodynamic force resulting from the fluid-structure interaction.

Following the derivation by Malaeb (1982), the stiffness is obtained by displacing the platform an arbitrary distance in the surge direction (Figure 12).

Summing the horizontal forces gives

$$kx = N(T_0 + \Delta T)\sin\psi \tag{3.2}$$

where k is the stiffness in the x-direction due to an arbitrary surge displacement, N is the number of tension legs, T_0 is the pretension of each leg and ΔT is the increase in tension per leg, given by

$$\Delta T = k_c \Delta d, \tag{3.3}$$

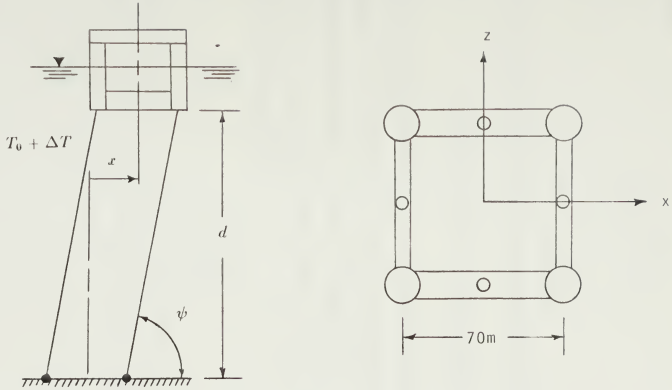

Figure 12. Schematic of a Tension Leg Platform.

where k_c is the equivalent stiffness per leg. In most cases ΔT is less than 20% of the pretension T_0. The change in cable length Δd and the angle of inclination ψ are given by

$$\Delta d = \sqrt{d^2 + x^2} - d, \tag{3.4}$$

and

$$\sin\psi = \frac{x}{\sqrt{d^2 + x^2}}. \tag{3.5}$$

Substituting equations (3.3) through (3.5) into Equation (3.2) gives

$$k = (T_0 + k_c\sqrt{d^2 + x^2} - k_c d)\frac{N}{\sqrt{d^2 + x^2}}. \tag{3.6}$$

Thus, the restoring force resulting from an arbitrary surge displacement is a function of the magnitude of the displacement as well as the material properties, pretension, and elongation of the tendons. The form of Equation (3.6) is that of a "hardening spring". When the surge displacement is small ($x << d$) Equation (3.6) can be reduced to a linear function of x:

$$k = \frac{NT_0}{d}. \tag{3.7}$$

The restoring force kx vs. x is plotted in Figure 13 using both Equations (3.6) and (3.7) with $k_c = 7.0(10^7)$ N/m, $T_0 = 4.8(10^7)$ N, and $d = 200$ m. The data listed in Table 1 are used for simulation purposes.

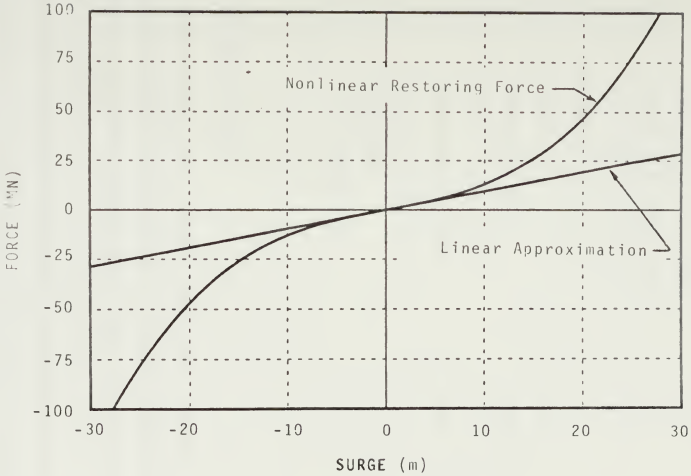

Figure 13. Tension Leg Platform Restoring Force.

Table 1. Typical TLP Data Based on Kirk and Etok (1979)

Structural Component	Dimensions
Diameter of 4 corner columns	16 m
Diameter of 4 middle columns	3.5 m
Diameter of 2 cross braces	6 m
Spacing of corner columns	70 m
Draft, h	35 m
Total mass in air, m	$5.4(10^7)$ kg
Fluid added mass in surge	$3.3(10^7)$ kg
Cable stiffness per leg, k_c	$7.0(10^7)$ N/m
Pretension of each leg, T_0	$10^7 - 10^8$ N
Water depth	200 – 1000 m
Critical damping ratio, ξ	0.00 – 0.15

B. Solution Procedure

The nonlinear equation of motion can be solved using one of several direct integration procedures. The Newmark-β method is chosen because of its well known convergence and stability criteria (Newmark, 1962). The Newmark-β equations are used to determine the velocity and displacement of the structure at time t_{i+1} based on the corresponding values at time t_i and the acceleration at time t_{i+1}. Since the value of the acceleration is not known a priori, an iterative procedure is required. The advantage of using such a procedure is that any nonlinearities, such as the TLP stiffness given by Equation (3.6), can easily be included in the analysis. The

Newmark-β equations are as follows:

$$\dot{x}_{i+1} = \dot{x}_i + (1-\gamma)\ddot{x}_i\Delta t + \gamma\ddot{x}_{i+1}\Delta t \tag{3.8}$$

and

$$x_{i+1} = x_i + \dot{x}_i\Delta t + (0.5-\beta)\ddot{x}_i(\Delta t)^2 + \beta\ddot{x}_{i+1}(\Delta t)^2 \tag{3.9}$$

where γ is taken as 0.5 to avoid spurious numerical damping and β is taken as 0.126 to ensure numerical stability with convergence (Newmark, 1962). The assumed value of $\ddot{x}_{i+1}$ is compared with the corresponding value calculated from the equation of motion:

$$\ddot{x}_{i+1} = \frac{1}{m}(F_{i+1} - c\dot{x}_{i+1} - kx_{i+1}). \tag{3.10}$$

Equations (3.8) through (3.10) are solved in an iterative manner until the assumed and calculated values of $\ddot{x}_{i+1}$ converge. The process is then repeated for subsequent time steps.

In order to ensure numerical stability, a two-pass procedure is used wherein the response of the TLP is first estimated using the relative motion form of the Morison equation. The drag and inertia force components are then filtered and superimposed using Equation (2.16) to obtain an adjusted force time series. This time series is then used as input to the Newmark-β algorithm, thus obtaining an adjusted response time series (Figure 14).

C. Simulation Results

The results from two typical numerical simulation cases are presented in Figures 15 through 24. In case one, the random wave profile is scaled such that the maximum wave height is approximately 10 meters. In case two, the same wave profile is used,

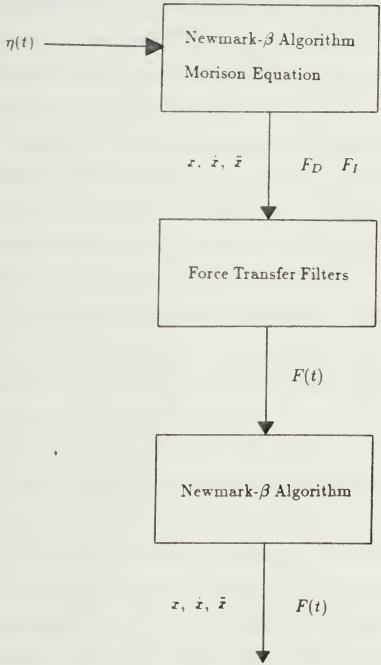

Figure 14. Response Simulation Flow Chart.

but scaled such that the maximum wave height is 30 meters. The force, surge, and tension time series are plotted after both the first and second pass of the Newmark-β algorithm. In both cases, the force transfer filters (2nd pass) result in a substantial increase in high frequency force components. These components are more pronounced when the wave height is small and the wave period is short. This may be due to the phase shift resulting from the spacing of the columns. If the wave length is equal to twice the column spacing (140 meters), then the resulting forces on opposing columns will partially cancel with one another. In all cases, the surge response is smooth because of the large inertia of the TLP. Since the variation in tension was represented as a function of the surge displacement by neglecting the dynamics of the tension legs, the tension time series is also smooth. If the dynamics of the tension legs were included by modeling the TLP as a MDOFS, then these high frequency force components should also occur in the tension time series. Such an analysis could explain the tension leg "ringing" phenomenon observed in the Hutton TLP model tests (Mercier, 1982).

Although, both cases produce similar results, the effect of the force transfer filters is more pronounced in case two where the maximum wave height is much greater than in case one. The principle limitation of the use of these filters is that the scale effect is unknown at this time. Like the Morison equation, the force transfer filters should be calibrated for a specific design application, taking into consideration the wave theory employed to estimate fluid particle kinematics, the ocean wave design spectra, and the size, shape, and interaction of the various structural components which comprise the platform.

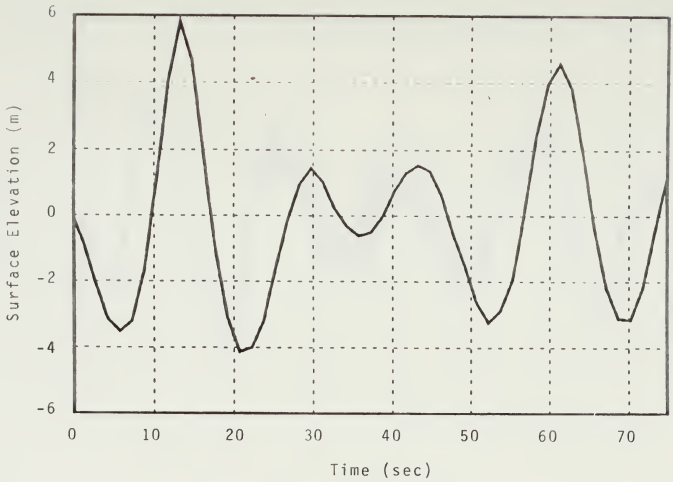

Figure 15. Surface Elevation – Case One.

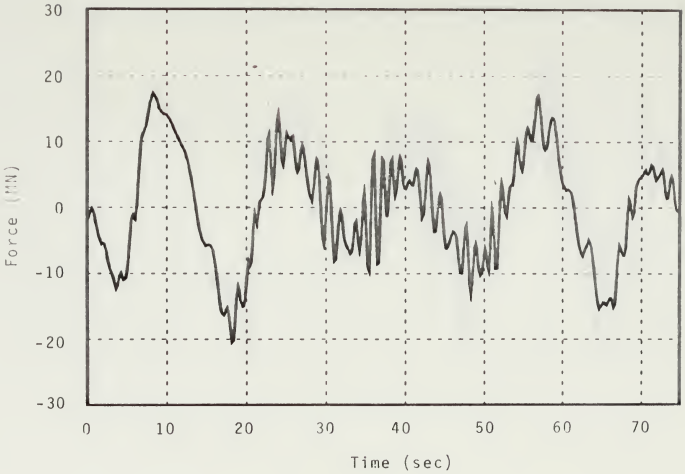

Figure 16. Force Using Morison Equation – Case One.

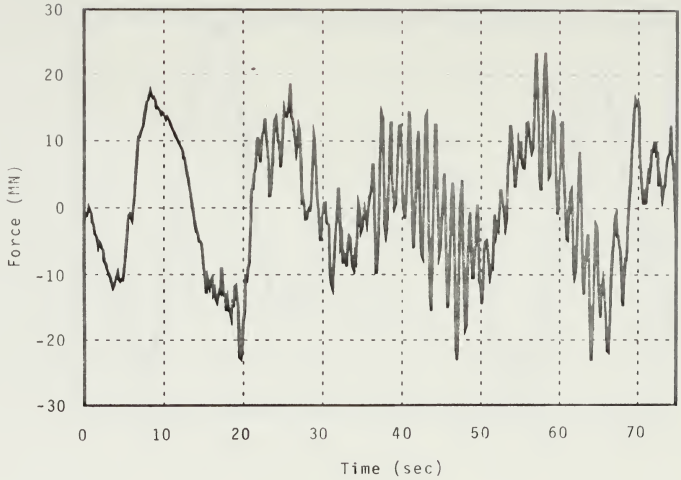

Figure 17. Force Using Filters – Case One.

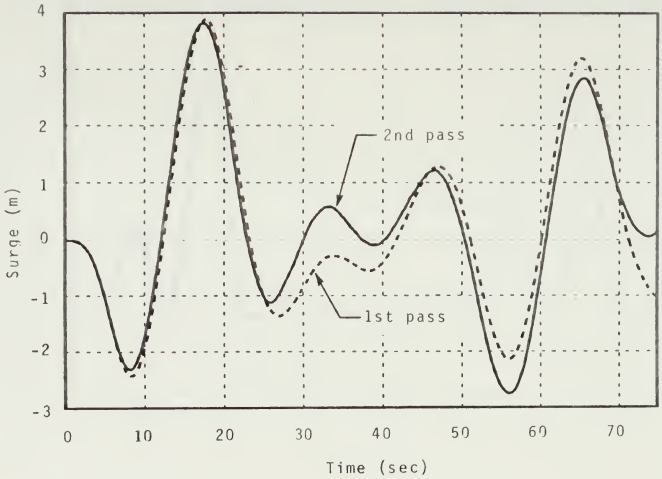

Figure 18. TLP Surge Response – Case One.

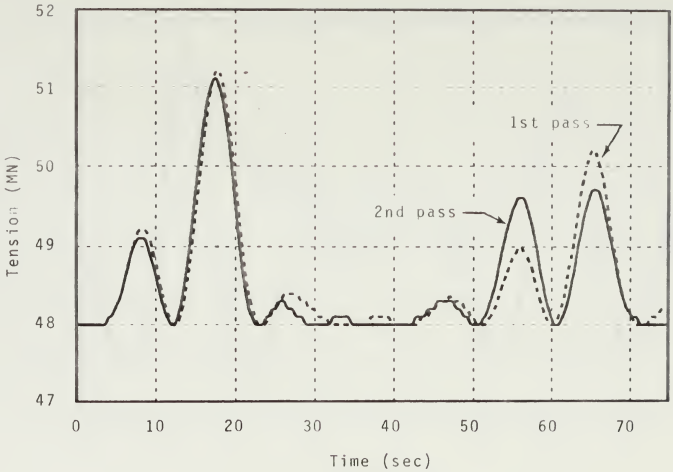

Figure 19. TLP Tension – Case One.

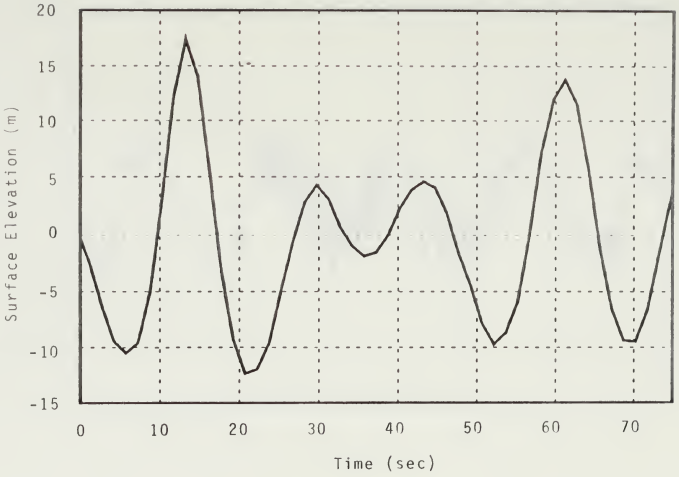

Figure 20. Surface Elevation – Case Two.

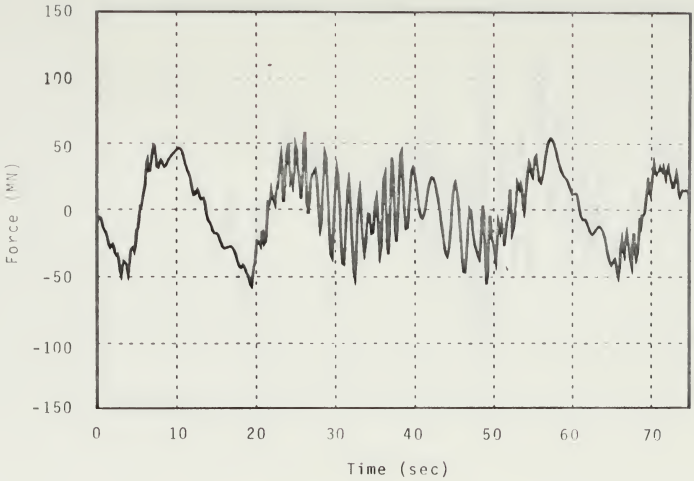

Figure 21. Force Using Morison Equation – Case Two.

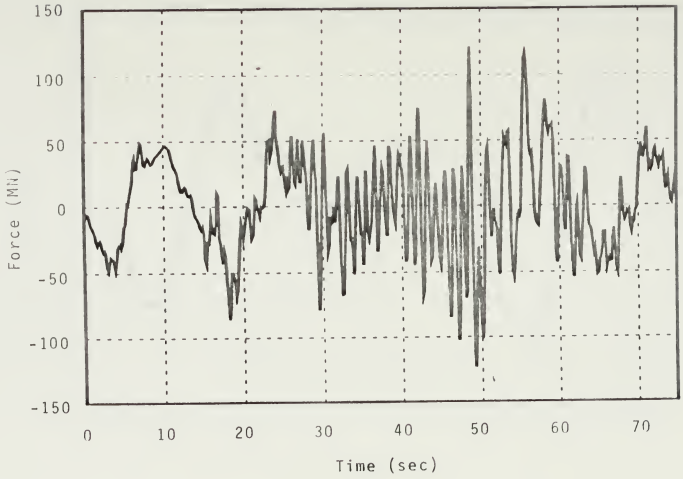

Figure 22. Force Using Filters – Case Two.

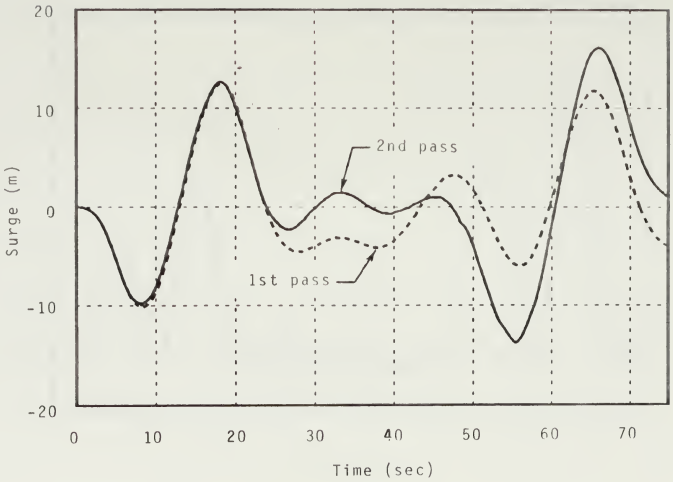

Figure 23. TLP Surge Response – Case Two.

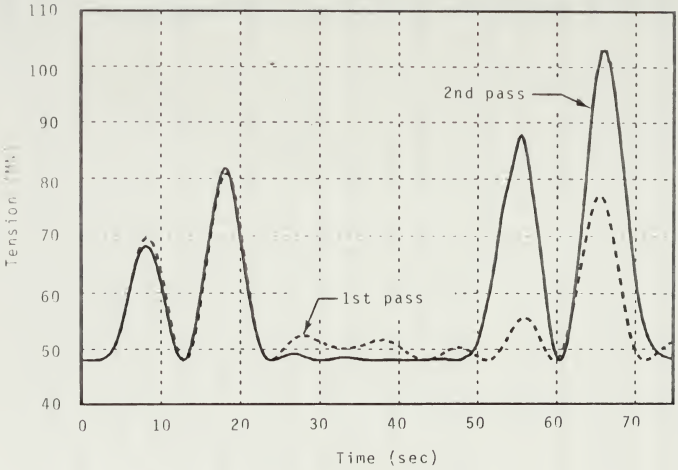

Figure 24. TLP Tension – Case Two.

CHAPTER IV

CONCLUSIONS

In this study, experimental data were analyzed to gain insight into the applications and limitations of the relative motion form of the Morison equation for the prediction of hydrodynamic forces on a free-to-surge vertical cylinder. A new force prediction procedure was presented to account for the effects of flow history on the instantaneous force. The following conclusions are made based upon this research:

(1) Small scale model tests suggest that the effect of flow history is significant in the prediction of hydrodynamic forces.

(2) The relative motion form of the Morison equation can not duplicate the high frequency force components measured in small scale model tests.

(3) In this study, the inclusion of explicit history terms captured the high frequency force components, increased the multiple correlation coefficient from 0.71 to 0.83, and decreased the root-mean-square error from 24% to 9%.

(4) The procedure to include history terms can be incorporated into the response simulation of more complex offshore structures such as the TLP.

The results from this research suggest that significant improvements in hydrodynamic force prediction can be obtained by including explicit history terms. A strong research effort is required to determine the scale effect on these history terms. Future research should include both large scale model tests and field data analysis. The results may prove to be of great importance in the fatigue analysis of offshore structures and may explain some of the variability between measured and calculated forces.

REFERENCES

[1] Aagaard, P.M. and Dean, R.G., "Wave Forces: Data Analysis and Engineering Calculation Method," in *Proceedings of the Offshore Technology Conference*, Houston, Texas, May 1969.

[2] Bird, A.R. and Mockros, L.F., "Measured Fluid Forces on an Accelerated/Decelerated Circular Cylinder," in *Proceedings of the Offshore Technology Conference*, Houston, Texas, May 1986.

[3] Borgman, L.E., "Statistical Models for Ocean Waves and Wave Forces," *Advances in Hydroscience*, Vol. 8, pp. 139-178, 1972.

[4] Dawson, T.H., "In-Line Forces on Vertical Cylinders in Deepwater Waves," in *Proceedings of the Offshore Technology Conference*, Houston, Texas, May 1984.

[5] Dawson, T.H.; Wallendorf, L.A.; and Hill, J.R., "Experimental Study of the Relative Motion Morison Equation," presented at the Ocean Structural Dynamics Symposium, Oregon State University, Corvallis, Oregon, September 1986.

[6] Dillingham, J.T., "Recent Experience in Model Scale Simulation of Tension Leg Platforms," *Marine Technology*, Vol. 21, No. 2, pp. 186-200, April 1984.

[7] Hamilton, W.S., "Fluid Force on Accelerating Bodies," in *Proceedings of the 13th Coastal Engineering Conference*, New York, New York, 1972.

[8] Keulegan, G.H. and Carpenter, L.H., "Forces on Cylinders and Plates in an Oscillating Fluid," *Journal of Research of the National Bureau of Standards*, Vol. 60, No. 5, pp. 423-440, 1958.

[9] Kirk, C.L. and Etok, E.U., "Dynamic Response of Tethered Production Platforms in a Random Sea State," in *Second International Conference on Behavior of Offshore Structures*, London, England, August 1979.

[10] Malaeb, D., "Dynamic Analysis of Tension-Leg Platforms," Ph.D. Dissertation, Texas A&M University, December 1982

[11] Mercier, J.A., "Evolution of Tension Leg Platform Technology," in *Behavior of Offshore Structures Conference*, Cambridge, Massachusetts, August 1982.

[12] Morison, J.R.; O'Brien, M.P.; Johnson, J.W.; and Schaaf, S.A., "The Forces Exerted by Surface Waves on Piles," *AIME Journal of Petroleum Transactions*, Vol. 189, pp. 149-157, 1950.

[13] Newmark, N.M., "A Method of Computation for Structural Dynamics," *ASCE Transactions*, Vol. 127, pp. 1406-1435, 1962.

[14] Newton, H.J., *TIMESLAB: A Time Series Analysis Laboratory*. Pacific Grove, California: Wadsworth & Brooks/Cole, 1988.

[15] Reid, R.O., "Correlation of Water Level Variation with Wave Forces on a Vertical Pile for Nonperiodic Waves," in *Proceedings of the VI Conference on Coastal Engineering*, Houston, Texas, 1958.

[16] Sarpkaya, T., "A Critical Assessment of Morison's Equation," in *International Symposium on Hydrodynamics in Ocean Engineering*, The Norwegian Institute of Technology, Trondheim, Norway, 1981.

[17] Sarpkaya, T. and Isaacson, M., *Mechanics of Wave Forces on Offshore Structures*. New York, New York: Van Nostrand Reinhold, 1981.

[18] Shields, D.R. and Hudspeth, R.T., "Hydrodynamic Force Model Research for Small Semisubmersibles," *Naval Civil Engineering Laboratory*, Technical Memorandum TM-44-85-06, September 1985.

[19] Wheeler, J.D., "Method for Calculating Forces Produced by Irregular Waves," in *Proceedings of the Offshore Technology Conference*, Houston, Texas, May 1969.

Supplemental Sources Consulted

[1] Dean, R.G. and Dalrymple, R.A., *Water Wave Mechanics for Engineers and Scientists*. Englewood Cliffs, New Jersey: Prentice-Hall, 1984.

[2] Paz, M., *Structural Dynamics: Theory and Computation*. New York, New York: Van Nostrand Reinhold, 2nd Ed., 1985.

APPENDIX A

NOMENCLATURE

A_n	amplitude of nth wave component
a	horizontal fluid particle acceleration
B	regression parameter vector
C_a	added mass coefficient
C_d	drag coefficient
C_m	inertia coefficient
C_3, C_5	remainder force Fourier coefficients
c	structural damping coefficient
c_{12}	cospectral density
D	diameter
d	length of tension leg at zero surge displacement
Δd	change in length of tension leg
F	total hydrodynamic force
F_D	hydrodynamic drag component
F_I	hydrodynamic inertia component
F_F	force resulting from the acceleration of fluid
f	hydrodynamic force per unit length
f_0	Nyquist frequency
g	acceleration of gravity
h	water depth
k	structural stiffness
k_c	equivalent stiffness per tension leg

k_n	wave number of nth wave component
l	maximum lag used in a filter i.e. memory length
m	mass of structure
N	number of tension legs
q_{12}	quadrature spectral density
R^2	multiple correlation coefficient
ΔR	remainder force i.e. error
T	wave period
T_0	pretension of each tension leg
ΔT	increase in tension per tension leg
t	time
Δt	change in time
$S(B)$	sum of the square of the errors
S_{11}, S_{22}	univariate spectral density
S_{12}	complex cross-spectral density
u	horizontal fluid particle velocity
W_{12}	coherency spectrum
X	regressor matrix
x, $\dot{x}$, $\ddot{x}$	surge displacement, velocity, and acceleration
y	response vector used in regression analysis
z	elevation from mean water level
α_k	drag filter coefficients
β	Newmark-β parameter
β_k	inertia filter coefficient
γ	Newmark-β parameter

ϵ	error time series
η	surface elevation time series
θ	nondimensionalized time defined as $\frac{2\pi t}{T}$
π	3.141...
ρ	fluid mass density
σ^2	sample variance
ϕ_n	phase angle of the nth wave component
ϕ_{12}	phase spectrum
ψ	angle of inclination in the xz plane
ω	frequency given by $\frac{k-1}{n}$ for $k = 1, \ldots, [\frac{n}{2}] + 1$
ω_n	frequency of the nth wave component
$\forall$	volume of displaced fluid

APPENDIX B

TIME SERIES ANALYSIS SOFTWARE

The statistical analysis results reported in this thesis were obtained using TIMESLAB. This computer program is essentially a time series analysis language consisting of approximately 150 commands. The software is provided with the text: *TIMESLAB: A Time Series Analysis Laboratory* (Newton, 1988). Some of the features which were used in this research include: regression with AR-errors, a test for white noise, auto- and cross-correlation, coherence and phase spectrum estimation, nonparametric spectral density estimation, and a test for statistical independence of two univariate realizations.

The TIMESLAB user can create files or "macros" containing commands. The macros used to estimate and plot the best-fit relative motion form of the Morison equation and the best-fit force transfer filters are provided below. Note that FILTERS.MAC calls another macro, REGAR.MAC, which is not listed here. REGAR.MAC is provided as part of the TIMESLAB software package.

```
;;
;;  FILTERS.MAC:    TIMESLAB macro to estimate and plot the best-fit relative
;;                  motion Morison equation and the best-fit force transfer
;;                  filters using regression with AR-errors.
;;
;;  Input:          y1      = total force
;;                  x1      = drag component
;;                  x2      = inertia component
;;                  i,j     = time window
;;                  maxlag  = maximum lag
;;
PAUSE
.start
;
n=j-i+1                                     ; regression parameters
m1={maxlag+1}*2
maxp=30
IF(maxp le m1,skip)
maxp=m1
;skip
;
y=EXTRACT(y1,i,j)                           ; instantaneous total force
x1lag=EXTRACT(x1,i,j)                       ; instantaneous drag force
x2lag=EXTRACT(x2,i,j)                       ; instantaneous inertia force
x=<x1lag,x2lag>                             ; form regressor matrix
;
m=2
MACRO(regar,start)                          ; regress on instantaneous values
LABEL(yy)='Morison Equation'
MAXMIN(y,n,ymax1,imax,ymin1,imin)
MAXMIN(yy,n,ymax2,imax,ymin2,imin)
yabs=ABS(ymin1)
ysave=y
y=y+yabs+ymax1
ysave1=y
LABEL(y)=' '
MAXMIN(y,n,ymax1,imax,ymin1,imin)
PLOTSIZE(480,120,55,30,8,10,8,1,0,0)
time=LINE(101,-0.15624,0.15624)
MACRO(error,start)
LABEL(time)='Time (sec).  Error=#err#%; R2=@R2@'
PLOTON
PLOT(time,y,n,0,16,ymin2,ymax1)             ; plot measured and predicted force
PLOT(time,yy,n,0,16,ymin2,ymax1)            ; using the Morison equation
PLOTOFF
Cd=beta[1]
Cm=beta[2]
LIST(Cd,Cm)                                 ; list drag and inertia coefficients
PROMPTOFF
;
m=m1
k=i
l=j
kmin=k-maxlag
;
;loop                                       ; loop to get lagged values
;
k=k-1
l=l-1
lag=i-k
LIST(lag)
x1lag=EXTRACT(x1,k,l)
x2lag=EXTRACT(x2,k,l)
X=<X,x1lag,x2lag>                           ; form regressor matrix
IF (k eq kmin,stop)                         ; using lagged values
GOTO (loop)
;
;stop                                       ; end of loop
;
```

```
y=ysave
CLEAN(x1lag,x2lag,k,1)
MACRO(regar,start)                          ; regress with history terms
:
LABEL(yy)='FTF with #lag# Lag Memory'
y=ysave1
LABEL(y)=  '
MAXMIN(yy,n,ymax2,imax,ymin2,imin)
MACRO(error,start)
LABEL(time)='Time (sec).  Error=#err#%; R2=@R2@'
PLOTON
PLOT(time,y,n,0,16,ymin2,ymax1)       ; plot measured and predicted force
PLOT(time,yy,n,0,16,ymin2,ymax1)      ; using the force transfer filters
PLOTOFF
PLOTSIZE(0)



::
::  ERROR:  Macro to compute the rms error and multiple correlation
::          coefficient.
::
::  Input:  ysave = Measured Force
::            yy  = Predicted
::             n  = length of arrays
::
PAUSE
;start
yrms=MMULT(ysave,ysave,1,n,1)
yrms=(yrms/n)*0.5
::
yyrms=MMULT(yy,yy,1,n,1)
yyrms=(yyrms/n)*0.5
::
mrms=yrms[1]
prms=yyrms[1]
clean(yrms,yyrms)
error=(mrms-prms)/mrms*100
err=0
err:=error
delta=error-err
IF(delta.lt.0.5,skip)
err=err+1
;skip
:
rho=CORR(res,n,30,0,1,se2,per)
rho=CORR(y,n,30,0,1,sy2,per)
R2=1.0-se2/sy2
```

VITA

Born in Seattle, Washington, Charles Blake Sajonia graduated from the University of Washington in May 1982 with a Bachelor of Science in Civil Engineering and was commissioned as an Ensign in the United States Navy Civil Engineer Corps. He has served with Amphibious Construction Battalion Two in Norfolk, Virginia, and as officer in charge of Construction Battalion Unit 409 in Long Beach, California. He commenced study towards a Master of Science in Ocean Engineering at Texas A&M University in January 1987.

Upon completion of his Master of Science degree, he will attend the Navy Diving and Salvage School in Panama City, Florida, and subsequently serve as the Hyperbaric Facilities Division Director at the Naval Medical Research Institute in Bethesda, Maryland.

His military awards include the Navy Commendation Medal, Navy Achievement Medal, and the Joint Meritorious Unit Award. He is a member of the American Society of Civil Engineers and the Society of American Military Engineers. His permanent address is 1325 North 44th Street, Seattle, Washington, 98103.

-897

Thesis
S152525 Sajonia
c.1 Random wave forces on
a free-to-surge vertical
cylinder.

Thesis
S152525 Sajonia
c.1 Random wave forces on
a free-to-surge vertical
cylinder.

GEMLU

thesS152525
Random wave forces on a free-to-surge ve
3 2768 000 78912 7
DUDLEY KNOX LIBRARY